

Integral equation and perturbation method of calculating thermodynamic functions for a square-well fluid

David D. Carley and Allen C. Dotson

Department of Physics, Western Michigan University, Kalamazoo, Michigan 49008

(Received 28 July 1980; revised manuscript received 3 November 1980)

The pressure of a classical simple fluid of particles interacting with square-well potentials is computed by a method combining the use of a parametric integral equation with first-order perturbation theory. This method leads to a simple expression for the pressure of the fluid. In contrast to the usual choice, the reference part of the potential energy is taken to be a square well itself. The results are in good agreement with pressure values from molecular dynamics and are relatively insensitive to the choice of the reference-well depth, provided that that well is shallow. Based on these findings, fine-meshed tables giving (reduced) pressure, internal energy, and Helmholtz free energy are constructed for ranges in reduced density and temperature of $n^* \leq 0.85$, $1.4 \leq T^* \leq 4.0$. These tables should provide reliable estimates of the thermodynamic variables for a square-well gas at any (n^*, T^*) within the given ranges; they also help to lay the basis for comparative studies of the applicability of perturbation theory to the square-well gas.

I. INTRODUCTION

This paper presents a study of a perturbation technique¹ for the calculation of thermodynamic functions for a square-well fluid in equilibrium. In particular, the method uses a parametric integral equation² to compute the radial distribution function³ for a reference system; this result is then combined with a perturbing potential to compute the pressure for a low-temperature square-well fluid. Comparisons with results from molecular dynamics⁴ enable us to study different separations of the potential energy into reference part and perturbation, and on this basis to construct tables of thermodynamic values. This approach, which has previously been applied in essence to a Lennard-Jones fluid,⁵ has an advantage in requiring relatively little computer time, as compared with that required for numerical simulations such as molecular dynamics, and at low temperatures and high densities is more accurate than the use of the integral equation directly. The tables obtained in the present work provide another setting in which this particular approach may be tested against numerical-simulation techniques, the results of which are often considered as standard.

Comparison of these tables with analogous ones from other perturbation techniques, with evaluation based on agreement with numerical-simulation results, may ultimately prove instructive. For example, a given potential energy function can be split into a reference part and a perturbation in different ways; studies of the relative success, in matching numerical-simulation results, of various different splittings may eventually improve our understanding of the conditions under which perturbation theories are successful. A comparative analysis of different splittings of

the Lennard-Jones potential has been made,⁶ and such an analysis of the square well may prove useful also.⁷ Thermodynamic tables could assist in this endeavor.

The most familiar decomposition of the square-well potential uses the hard core as the reference potential and the attractive part as the perturbation.⁸ However, we show that good values of pressure can be obtained by using, as the reference part, a square well of lesser depth than the given one. Moreover, changing the relative depths of these wells is found to affect the pressure values only weakly (as one would hope), as long as the reference well is kept relatively shallow. These results suggest that, with a proper choice of relative well depths, this approach can lead to reliable thermodynamic tables for the square-well gas. We present tables for reduced pressure, internal energy, and Helmholtz free energy, and we compare interpolations based on the internal energy table to values obtained from molecular dynamics.

II. DECOMPOSITION OF THE POTENTIAL

We take as our system N particles in a volume V which interact such that the potential energy of the system is a sum of pair interaction energies of the form

$$\phi(r) = \begin{cases} \infty, & r < d \\ -\epsilon, & d \leq r \leq 1.5d \\ 0, & r > 1.5d \end{cases} \quad (1)$$

where ϕ is the pair potential energy, r is the particle separation distance, ϵ is the well depth, and d is the diameter of the hard-sphere core. The system pair potential function is separated into the sum of a reference potential (ϕ_r) and a

perturbing potential (ϕ_p) so that

$$\phi = \phi_p + \phi_r. \quad (2)$$

We take the reference potential to be

$$\phi_r(r) = \begin{cases} \infty, & r < d \\ -\alpha\epsilon, & d \leq r \leq 1.5d \\ 0, & r > 1.5d \end{cases} \quad (3)$$

where α , the relative depth of the reference-potential well, falls in the range $0 \leq \alpha \leq 1$. We introduce the quantities

$$\begin{aligned} x &= r/d, \\ T^* &= kT/\epsilon, \\ T^+ &= T^*/\alpha, \\ \beta &= 1/kT, \end{aligned} \quad (4)$$

where k is Boltzmann's constant and T is the absolute temperature. We then have

$$\beta\phi = \begin{cases} \infty, & \text{for } x < 1 \\ -1/T^*, & \text{for } 1 \leq x \leq 1.5 \\ 0, & \text{for } x > 1.5 \end{cases} \quad \beta\phi_r = \begin{cases} \infty, & \text{for } x < 1 \\ -1/T^+, & \text{for } 1 \leq x \leq 1.5 \\ 0, & \text{for } x > 1.5 \end{cases} \quad (5)$$

Thus we see that the reference potential is also a square well of the same form, but of less depth than the system well when we take $T^+ > T^*$.

III. PRESSURE COMPUTATIONS USING DIFFERENT REFERENCE-WELL DEPTHS

The direct perturbation-theory approach to calculating pressure begins with obtaining the radial distribution function and the pressure values for the reference system. Then the Helmholtz free energy (F) of the given system is given, from first-order perturbation theory, by

$$F = F_r + F_p = F_r + \frac{N^2}{2V} \int_0^\infty g_r(r) \phi_p(r) 4\pi r^2 dr, \quad (6)$$

where g_r is the reference system's radial distribution function. We introduce the dimensionless quantities

$$\begin{aligned} n^* &= Nd^3/V, \\ P^* &= pV/NkT, \\ F^* &= 2F/3NkT, \\ U^* &= 2U/3NkT, \end{aligned} \quad (7)$$

where p is the pressure and U is the internal energy. Equation (6) can then be written as

$$F^* = F_r^* + F_p^* = F_r^* + \frac{4\pi n^*(\alpha-1)}{3T^*} \int_1^{1.5} g_r(x)x^2 dx. \quad (8)$$

We note the thermodynamic relationship

$$dF^* = \left(\frac{2P^*}{3n^*} \right) dn^* - \left(\frac{U^*}{T^*} \right) dT^*, \quad (9)$$

from which it follows that⁵

$$P^* = P_r^* + \frac{3n^*}{2} \left(\frac{\partial F_p^*}{\partial n^*} \right)_{T^*}. \quad (10)$$

One can thus obtain the desired pressure values from the P_r^* values and the F_p^* values given, in terms of $g_r(x)$, by Eq. (8).

However, radial distribution functions and Padé-approximant forms for pressure have been obtained previously,⁹ by use of a parametric integral equation, for a square-well gas at the four reduced temperatures of 3.3333, 6.11, 10.0, and 20.0. Moreover, comparison of Eq. (8) with the square-well formula⁹ for internal energy,

$$U^*(n^*, T^*) = 1 - \frac{4\pi n^*}{3T^*} \int_1^{1.5} g(x)x^2 dx, \quad (11)$$

shows that

$$F_p^*(n^*, T^*) = (\alpha - 1) \left(\frac{T^+}{T^*} \right) [1 - U_r^*(n^*, T^+)]$$

and Padé-approximant forms at the four temperatures (now taken as T^+ values) were reported in Ref. 9 for U^* , also. Thus pressure values for the actual system can easily be computed from the equations

$$\begin{aligned} P^* &= P_r^* - \frac{3n^*}{2} (\alpha - 1) \left(\frac{T^+}{T^*} \right) \frac{\partial U_r^*}{\partial n^*}, \\ P_r^* &= \frac{(1 + a_1 n^* + a_2 n^{*2} + a_3 n^{*3})}{(1 + a_4 n^* + a_5 n^{*2} + a_6 n^{*3})}, \\ U_r^* &= \frac{(1 + b_1 n^* + b_2 n^{*2} + b_3 n^{*3})}{(1 + b_4 n^* + b_5 n^{*2} + b_6 n^{*3})}, \end{aligned} \quad (12)$$

where T^*/T^+ can be substituted for α , and the Padé-approximant coefficients are given in Ref. 9 for each choice of T^+ .

In these calculations there are two fundamental sources of error: (1) the approximate integral equation used to compute the reference radial distribution functions, and (2) the perturbation equation [Eq. (6)], which ignores terms beyond first order. The parametric integral equation, for a parameter depending only upon the temperature, works best for shallow potential wells. However, the more shallow the reference-potential well, the greater is the perturbation and presumably, the greater the contribution of the higher-order terms in the perturbation series. By varying the reference temperature T^+ it is possible to study the effect of varying the perturbation strength. If the system pressure depends strongly upon T^+ , then clearly the method is not useful.

However, if the pressure is not strongly dependent upon T^* , it is at least an indication that the approximations introduce only small errors.

We have chosen to study the isotherms $T^*=2.0$ (gas), $T^*=1.4$ (slightly above the critical temperature), $T^*=1.0$ (liquid-vapor), and $T^*=0.7$ (liquid-vapor). The results of the calculation of P^* as a function of n^* are shown in Figs. 1-4 and are compared with simulation results estimated from the calculations⁴ of Alder, Young, and Mark. It may be seen that P^* does depend somewhat upon the separation of the potential (value of T^*), but that there is relatively good agreement between results obtained using $T^*=20, 10, 6.11$, and the simulation values. Presumably, the values for $T^*=3.33$ are not as good because the integral equation (as used) becomes less reliable for lower values of T^* .

Using Eqs. (12), values of P^* are computed, over a range in T^* , at each of several densities at which Alder, Young, and Mark have reported values; these P^* vs T^* graphs are obtained for each of the four T^* choices available. Figures 5-8 show that there is good agreement with molecular-dynamics results when T^* is chosen as 6.11. Since this choice for T^* lies in the range for which P^* results are, as desired, relatively insensitive to the value of T^* , we set the reference temperature at 6.11 for the rest of the computations.

IV. COMPUTATIONS FOR THE THERMODYNAMIC TABLES

We construct tables of P^* , U^* , and F^* , since other thermodynamic functions are easily obtained from these three. Values are given at intervals of 0.05 in n^* and 0.2 in T^* , in order to permit

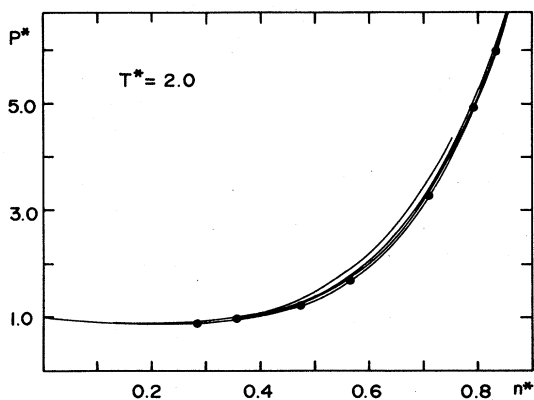


FIG. 1. The pressure (P^*) is plotted as a function of density (n^*) for a temperature (T^*) of 2.0. The solid curves represent perturbation results using T^* values of 3.3333, 6.11, 10.0, and 20.0 (top curve to bottom curve). The points are molecular-dynamics results estimated from the data of Alder, Young, and Mark.

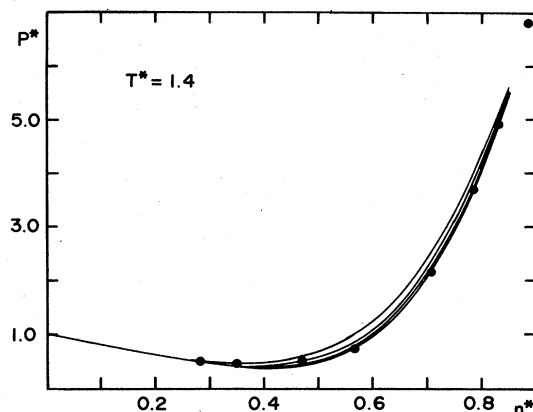


FIG. 2. The pressure (P^*) is plotted as a function of density (n^*) for a temperature (T^*) of 1.4. The solid curves represent perturbation results using T^* values of 3.3333, 6.11, 10.0, and 20.0 (top curve to bottom curve). The points are molecular-dynamics results estimated from the data of Alder, Young, and Mark.

reliable interpolations within the chosen ranges of $n^* \leq 0.85$, $1.4 \leq T^* \leq 4.0$. The overall procedure for developing the tables can be summarized as follows.

A. Calculation of P^* at $n^* \geq 0.20$

First we calculate P^* for $n^*=0.20, 0.25, 0.30, \dots, 0.85$, for each of the temperatures $T^*=1.4, 1.6, 1.8, \dots, 4.0$. These computations are done as described in Sec. III, with $T^*=6.11$ in Eqs. (12).

B. Calculation of P^* and U^* at $n^* \leq 0.20$

For the lower densities $n^*=0.001, 0.05, 0.10, 0.15$, and 0.20, and at each temperature T^* listed

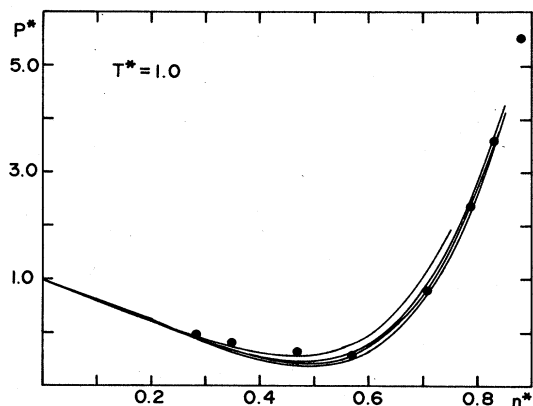


FIG. 3. The pressure (P^*) is plotted as a function of density (n^*) for a temperature (T^*) of 1.0. The solid curves represent perturbation results using T^* values of 3.3333, 6.11, 10.0, and 20.0 (top curve to bottom curve). The points are molecular-dynamics results estimated from the data of Alder, Young, and Mark.

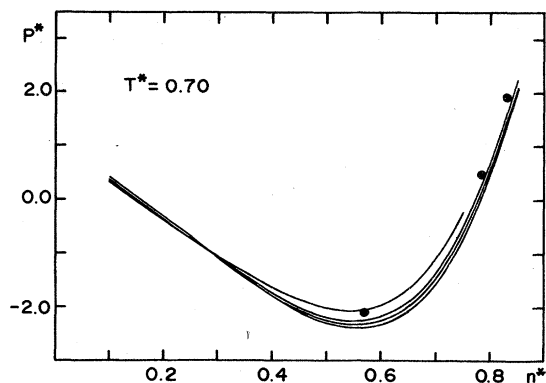


FIG. 4. The pressure (P^*) is plotted as a function of density (n^*) for a temperature (T^*) of 0.7. The solid curves represent perturbation results using T^* values of 3.3333, 6.11, 10.0, and 20.0 (top curve to bottom curve). The points are molecular-dynamics results estimated from the data of Alder, Young, and Mark.

in Sec. IV A, we solve the Percus-Yevick equation for the radial distribution function $g(x)$ and from it obtain P^* and U^* . At low densities, integral-equation techniques give more reliable values than perturbation theory, and the Percus-Yevick method is a simple technique to employ. At the common density $n^*=0.20$, the P^* values from Sec. IV A are all within ± 0.03 of the Percus-Yevick results, and all but two (at $T^*=1.4$ and 1.6) are within ± 0.01 of them.

C. Calculation of F^* at $n^*=0.001$

Based upon an arbitrary base value F_o^* chosen for the state ($n^*=0.001$, $T^*=20.0$), we calculate $F^*(0.001, T^*)$ for each of the temperatures T^* listed in Sec. IV A. The method⁹ is to integrate

$$dF^* = \left(\frac{2P^*}{3n^*}\right)dn^* - \left(\frac{U^*}{T^*}\right)dT^* \quad (9)$$

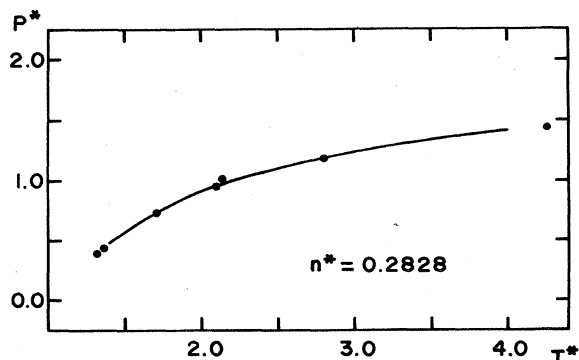


FIG. 5. The pressure (P^*) is plotted as a function of temperature (T^*) for a density (n^*) of 0.2828. The solid curve represents results from the present method, and the points are molecular-dynamics results from Alder, Young, and Mark.

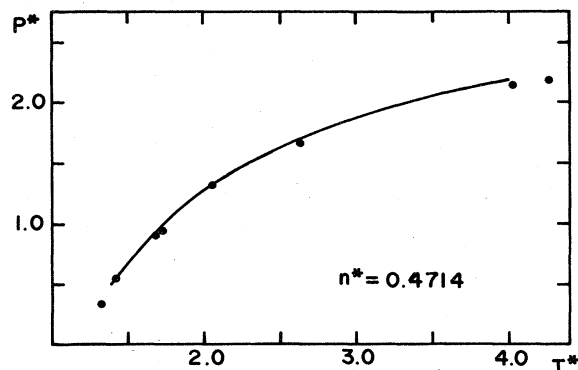


FIG. 6. The pressure (P^*) is plotted as a function of temperature (T^*) for a density (n^*) of 0.4714. The solid curve represents results from the present method, and the points are molecular-dynamics results from Alder, Young, and Mark.

along the line $n^*=0.001$. Along this line, $g(x)$ is very nearly equal to $e^{-\beta\phi}$, which, when substituted into Eq. (11), leads to the simple approximate equation,

$$U^* \approx 1 - \frac{9.5\pi n^*}{9T^*}. \quad (13)$$

Thus the F^* values are obtained from

$$F^*(0.001, T^*) = F_o^* - \int_{20.0}^{T^*} \left(1 - \frac{9.5 \times 10^{-3}\pi}{9T^*}\right) \frac{dT^*}{T^*}. \quad (14)$$

D. Calculation of F^* at $n^* > 0.001$

The method⁹ now is to apply Eq. (9) to isotherms at each of the temperatures T^* listed in Sec. IV A, resulting in

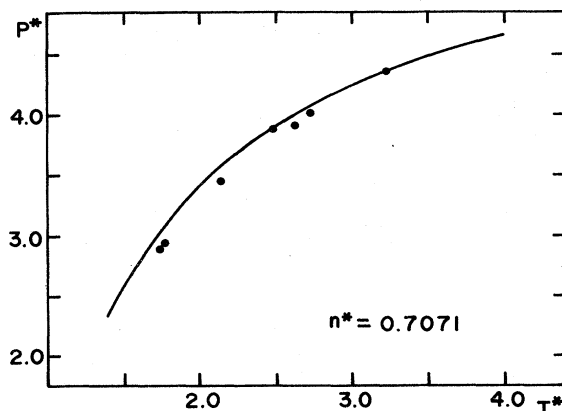


FIG. 7. The pressure (P^*) is plotted as a function of temperature (T^*) for a density (n^*) of 0.7071. The solid curve represents results from the present method, and the points are molecular-dynamics results from Alder, Young, and Mark.

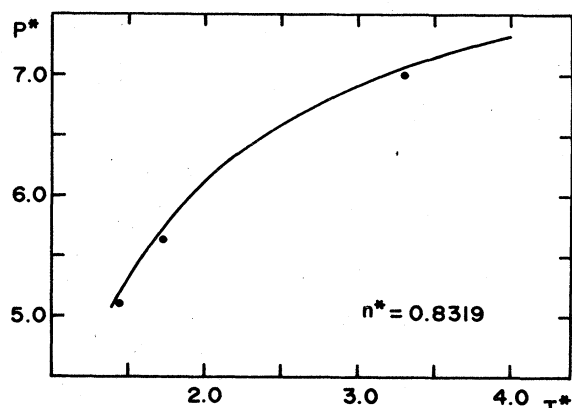


FIG. 8. The pressure (P^*) is plotted as a function of temperature (T^*) for density (n^*) of 0.8319. The solid curve represents results from the present method, and the points are molecular-dynamics results from Alder, Young, and Mark.

$$F^*(n^*, T^*) = F^*(0.001, T^*) + \int_{0.001}^{n^*} \left(\frac{2P^*}{3n^*} \right) dn^*. \quad (15)$$

In these integrations, the values used for P^* are obtained in two different ways. The Percus-Yevick results of Sec. IV B form the basis of the P^* data in the lower density range ($n^* \leq 0.20$): the values used are interpolated, assuming the form

$$P^* = 1 + c_1 n^* + c_2 n^{*2} + c_3 n^{*3}. \quad (16)$$

For the higher densities, the P^* values of Sec. IV A are interpolated by use of the (3, 3) Padé-approximant form,

$$P^* = \frac{1 + d_1 n^* + d_2 n^{*2} + d_3 n^{*3}}{1 + d_4 n^* + d_5 n^{*2} + d_6 n^{*3}}. \quad (17)$$

The reason for not using perturbation-theory values for P^* throughout the integration is that Percus-Yevick values are more reliable at low densities. It is particularly important to use ac-

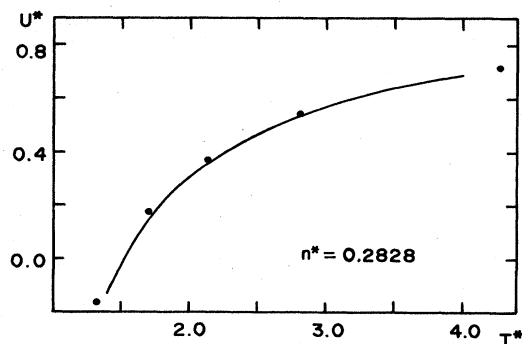


FIG. 9. The internal energy (U^*) is plotted as a function of temperature (T^*) for a density (n^*) of 0.2828. The solid curve represents results from the present method, and the points are molecular-dynamics results from Alder, Young, and Mark.

TABLE I. The pressure (P^*) for a square-well gas as a function of density (n^*) and temperature (T^*).

n^*	$T^*=1.4$	$T^*=1.6$	$T^*=1.8$	$T^*=2.0$	$T^*=2.2$	$T^*=2.4$	$T^*=2.6$	$T^*=2.8$	$T^*=3.0$	$T^*=3.2$	$T^*=3.4$	$T^*=3.6$	$T^*=3.8$	$T^*=4.0$
0.001	0.996912	0.997779	0.998402	0.998870	0.999234	0.999525	0.999763	0.999961	1.000128	1.000271	1.000395	1.000503	1.000599	1.000683
0.05	0.86	0.90	0.93	0.95	0.97	0.98	0.99	1.00	1.01	1.02	1.02	1.03	1.03	1.04
0.10	0.74	0.82	0.87	0.91	0.95	0.98	1.00	1.02	1.03	1.05	1.06	1.07	1.08	1.09
0.15	0.64	0.75	0.83	0.89	0.94	0.98	1.02	1.04	1.07	1.09	1.11	1.12	1.14	1.15
0.20	0.58	0.72	0.81	0.89	0.96	1.01	1.05	1.09	1.12	1.15	1.17	1.19	1.21	1.23
0.25	0.53	0.68	0.80	0.90	0.98	1.04	1.10	1.14	1.18	1.22	1.25	1.28	1.31	1.33
0.30	0.46	0.65	0.80	0.92	1.02	1.10	1.17	1.22	1.27	1.32	1.36	1.39	1.42	1.45
0.35	0.42	0.65	0.83	0.97	1.08	1.18	1.26	1.33	1.39	1.45	1.50	1.54	1.57	1.61
0.40	0.41	0.68	0.89	1.06	1.19	1.31	1.40	1.48	1.56	1.62	1.67	1.72	1.77	1.80
0.45	0.46	0.76	1.00	1.19	1.35	1.48	1.59	1.68	1.77	1.84	1.90	1.96	2.01	2.05
0.50	0.57	0.92	1.18	1.40	1.57	1.72	1.84	1.95	2.04	2.12	2.19	2.26	2.31	2.36
0.55	0.78	1.16	1.45	1.69	1.88	2.04	2.18	2.29	2.40	2.48	2.56	2.63	2.69	2.75
0.60	1.11	1.51	1.83	2.09	2.29	2.47	2.61	2.74	2.85	2.94	3.03	3.10	3.17	3.23
0.65	1.58	2.01	2.35	2.61	2.83	3.02	3.17	3.30	3.42	3.52	3.61	3.69	3.76	3.82
0.70	2.23	2.68	3.02	3.30	3.53	3.72	3.88	4.01	4.13	4.24	4.33	4.41	4.48	4.55
0.75	3.10	3.55	3.90	4.18	4.40	4.60	4.76	4.89	5.01	5.12	5.21	5.29	5.37	5.43
0.80	4.21	4.65	5.00	5.27	5.50	5.69	5.85	5.98	6.10	6.20	6.29	6.37	6.45	6.51
0.85	5.62	6.04	6.37	6.63	6.85	7.03	7.18	7.31	7.43	7.53	7.61	7.69	7.76	7.82

TABLE II. The internal energy (U^*) for a square-well gas as a function of density (n^*) and temperature (T^*).

n^*	$T^*=1.4$	$T^*=1.6$	$T^*=1.8$	$T^*=2.0$	$T^*=2.2$	$T^*=2.4$	$T^*=2.6$	$T^*=2.8$	$T^*=3.0$	$T^*=3.2$	$T^*=3.4$	$T^*=3.6$	$T^*=3.8$	$T^*=4.0$
0.001	0.995163	0.996129	0.996790	0.997267	0.997626	0.997905	0.998127	0.998308	0.998457	0.998584	0.998691	0.998784	0.998865	0.998935
0.05	0.76	0.81	0.84	0.87	0.88	0.90	0.91	0.92	0.92	0.93	0.93	0.94	0.94	0.95
0.10	0.54	0.63	0.69	0.74	0.77	0.80	0.82	0.83	0.85	0.86	0.87	0.88	0.89	0.89
0.15	0.33	0.46	0.55	0.61	0.66	0.70	0.73	0.75	0.77	0.79	0.80	0.82	0.83	0.84
0.20	0.14	0.31	0.42	0.49	0.55	0.60	0.64	0.67	0.70	0.72	0.74	0.75	0.77	0.78
0.25	-0.02	0.16	0.29	0.38	0.45	0.51	0.55	0.59	0.62	0.65	0.67	0.69	0.71	0.73
0.30	-0.19	0.02	0.16	0.27	0.35	0.41	0.46	0.51	0.55	0.58	0.61	0.63	0.65	0.67
0.35	-0.36	-0.13	0.03	0.15	0.24	0.31	0.37	0.42	0.47	0.50	0.53	0.56	0.59	0.61
0.40	-0.53	-0.29	-0.11	0.02	0.13	0.21	0.28	0.33	0.38	0.42	0.46	0.49	0.52	0.55
0.45	-0.71	-0.44	-0.25	-0.10	0.01	0.10	0.18	0.24	0.30	0.35	0.39	0.42	0.46	0.49
0.50	-0.90	-0.60	-0.39	-0.23	-0.10	0.00	0.08	0.15	0.21	0.27	0.31	0.35	0.39	0.42
0.55	-1.08	-0.77	-0.53	-0.36	-0.22	-0.11	-0.02	0.06	0.13	0.19	0.24	0.28	0.32	0.36
0.60	-1.26	-0.93	-0.67	-0.49	-0.34	-0.22	-0.12	-0.03	0.04	0.11	0.16	0.21	0.25	0.29
0.65	-1.44	-1.08	-0.81	-0.61	-0.45	-0.32	-0.21	-0.12	-0.04	0.03	0.09	0.14	0.19	0.23
0.70	-1.61	-1.23	-0.95	-0.73	-0.56	-0.42	-0.31	-0.21	-0.12	-0.05	0.02	0.07	0.12	0.17
0.75	-1.78	-1.38	-1.08	-0.85	-0.67	-0.52	-0.39	-0.29	-0.20	-0.12	-0.05	0.01	0.06	0.11
0.80	-1.93	-1.51	-1.20	-0.96	-0.76	-0.61	-0.48	-0.36	-0.27	-0.19	-0.12	-0.05	0.01	0.05
0.85	-2.07	-1.64	-1.30	-1.06	-0.85	-0.69	-0.55	-0.43	-0.34	-0.25	-0.17	-0.10	-0.05	0.00

TABLE III. The Helmholtz free energy (F^*) of a square-well gas as a function of the density (n^*) and temperature (T^*). Values are relative to the value (F_0^*) at $n^*=0.001, T^*=20.0$.

n^*	$T^*=1.4$	$T^*=1.6$	$T^*=1.8$	$T^*=2.0$	$T^*=2.2$	$T^*=2.4$	$T^*=2.6$	$T^*=2.8$	$T^*=3.0$	$T^*=3.2$	$T^*=3.4$	$T^*=3.6$	$T^*=3.8$	$T^*=4.0$
0.001	2.65597	2.52302	2.40565	2.30060	2.20554	2.11872	2.03884	1.96486	1.89598	1.83154	1.77099	1.71391	1.65990	1.60867
0.05	5.1665	5.0613	4.9638	4.8737	4.7904	4.7129	4.6407	4.5731	4.5096	4.4498	4.3933	4.3398	4.2889	4.2404
0.10	5.5368	5.4585	5.3802	5.3047	5.2328	5.1646	5.1000	5.0388	4.9808	4.9257	4.8733	4.8233	4.7756	4.7300
0.15	5.7236	5.6705	5.6105	5.5489	5.4880	5.4288	5.3717	5.3168	5.2642	5.2137	5.1654	5.1190	5.0745	5.0317
0.20	5.8411	5.8111	5.7682	5.7199	5.6697	5.6192	5.5694	5.5207	5.4734	5.4277	5.3834	5.3406	5.2993	5.2594
0.25	5.9261	5.9162	5.8890	5.8532	5.8132	5.7713	5.7287	5.6862	5.6443	5.6032	5.5631	5.5240	5.4860	5.4490
0.30	5.9864	5.9973	5.9862	5.9634	5.9340	5.9009	5.8658	5.8297	5.7933	5.7571	5.7212	5.6859	5.6513	5.6174
0.35	6.0315	6.0639	6.0695	6.0600	6.0415	6.0175	5.9901	5.9607	5.9300	5.8988	5.8673	5.8360	5.8049	5.7742
0.40	6.0683	6.1227	6.1454	6.1497	6.1424	6.1278	6.1083	6.0856	6.0608	6.0347	6.0078	5.9805	5.9530	5.9255
0.45	6.1021	6.1790	6.2192	6.2375	6.2417	6.2366	6.2252	6.2095	6.1907	6.1698	6.1476	6.1244	6.1006	6.0764
0.50	6.1377	6.2374	6.2955	6.3280	6.3438	6.3484	6.3452	6.3365	6.3238	6.3083	6.2908	6.2717	6.2517	6.2309
0.55	6.1799	6.3027	6.3786	6.4254	6.4529	6.4673	6.4723	6.4707	6.4641	6.4540	6.4412	6.4263	6.4100	6.3926
0.60	6.2338	6.3794	6.4730	6.5341	6.5733	6.5973	6.6106	6.6160	6.6155	6.6107	6.6026	6.5919	6.5794	6.5653
0.65	6.3045	6.4725	6.5837	6.6586	6.7092	6.7428	6.7641	6.7764	6.7819	6.7823	6.7789	6.7723	6.7634	6.7527
0.70	6.3977	6.5874	6.7154	6.8039	6.8655	6.9083	6.9374	6.9563	6.9676	6.9731	6.9741	6.9715	6.9661	6.9586
0.75	6.5193	6.7296	6.8736	6.9748	7.0470	7.0985	7.1350	7.1603	7.1770	7.1874	7.1926	7.1937	7.1917	7.1873
0.80	6.6753	6.9048	7.0637	7.1770	7.2589	7.3185	7.3620	7.3932	7.4150	7.4299	7.4392	7.4438	7.4449	7.4433
0.85	6.8724	7.1195	7.2921	7.4163	7.5072	7.5743	7.6242	7.6607	7.6872	7.7062	7.7191	7.7269	7.7308	7.7319

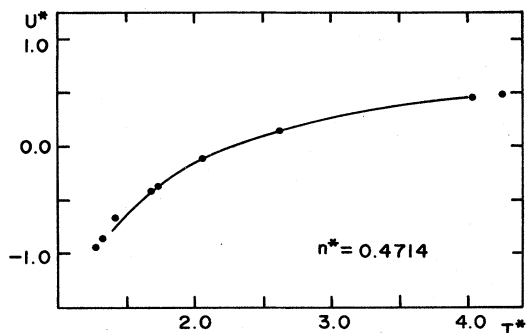


FIG. 10. The internal energy (U^*) is plotted as a function of temperature (T^*) for a density (n^*) of 0.4714. The solid curve represents results from the present method, and the points are molecular-dynamics results from Alder, Young, and Mark.

curate P^* values in the low-density region since they are divided, in Eq. (15), by small values of n^* . As mentioned at the end of Sec. IV B, the two sets of P^* values join smoothly at $n^*=0.20$.

E. Calculation of U^* at $n^* \geq 0.20$

Finally the remaining U^* values are computed from Eq. (9), as applied to a line along which n^* is constant⁵:

$$U^* = -T^* \left(\frac{\partial F^*}{\partial T^*} \right). \quad (18)$$

The U^* values at $n^*=0.20$ obtained in this procedure agree with those calculated in Sec. IV B to within ± 0.01 .

The resulting tables for P^* , U^* , and F^* are given as Tables I, II, and III. At the overlap density $n^*=0.20$, Percus-Yevick results are given.

V. FURTHER COMPARISONS WITH MOLECULAR DYNAMICS RESULTS, AND CONCLUSIONS

We can now make additional comparisons with the results of Alder, Young, and Mark. Using

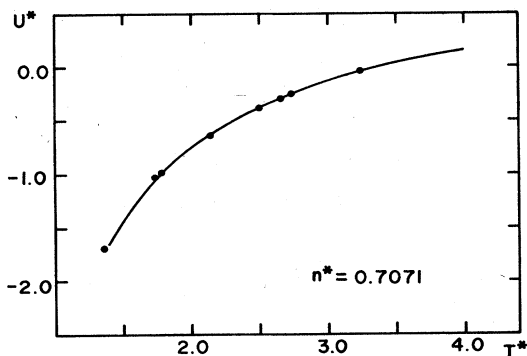


FIG. 11. The internal energy (U^*) is plotted as a function of temperature (T^*) for a density (n^*) of 0.7071. The solid curve represents results from the present method, and the points are molecular-dynamics results from Alder, Young, and Mark.

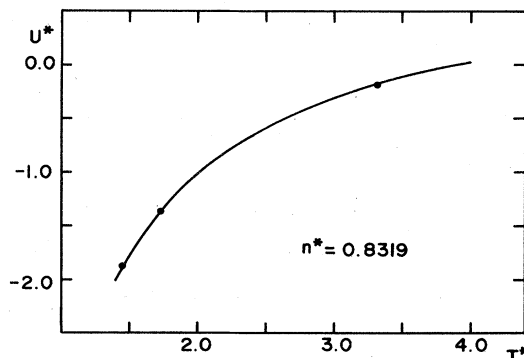


FIG. 12. The internal energy (U^*) is plotted as a function of temperature (T^*) for a density (n^*) of 0.8319. The solid curve represents results from the present method, and the points are molecular-dynamics results from Alder, Young, and Mark.

(3, 3) Padé approximants based on our table for U^* , we interpolate to obtain U^* values at those same densities as were used to compare P^* values. Figures 9–12 show the comparisons for U^* . In summary, the agreement of the present method's results with those of molecular dynamics is found to be very good for U^* at all four densities tried and for P^* at the lower ones, and agreement is fairly good for P^* at the higher densities.

It is well known that integral equations give reliable results at low densities, whereas perturbation theories tend to work well at high densities. At least as early as 1969, the idea of incorporating the relative strengths of these two approaches into a single theory was advanced.¹⁰ This paper has reported on one method of making such a combination, as applied to the construction of fine-meshed thermodynamic tables for a square-well gas. Since only one parameter (T^*) was adjusted to maximize agreement with molecular dynamics results, and since the results obtained here are not highly dependent even on that one specification, the overall agreement as indicated in the figures suggests that this method is reliable for the given system of interest. The resulting tables, therefore, permit trustworthy values of the thermodynamic functions to be calculated for the square-well gas described by Eq. (1), in the (n^* , T^*) range given by ($n^* \leq 0.85$, $1.4 \leq T^* \leq 4.0$). Moreover, in any comparative analysis of decompositions of the square-well potential, these tables may be taken as adequately describing the thermodynamic implications of using, as discussed in this paper, a shallow square well as the reference potential.

ACKNOWLEDGMENT

Computations were performed on the DEC PDP 10 computer at the Western Michigan University Computer Center.

- ¹R. W. Zwanzig, *J. Chem. Phys.* 22, 1420 (1954).
- ²D. D. Carley, *Phys. Rev. A* 10, 863 (1974).
- ³A discussion of the radial distribution function, perturbation theory, and calculation of thermodynamic functions can be found in the book, D. A. McQuarrie, *Statistical Mechanics* (Harper and Row, New York, 1976).
- ⁴B. J. Alder, D. A. Young, and M. A. Mark, *J. Chem. Phys.* 56, 3013 (1972).
- ⁵D. D. Carley, *J. Chem. Phys.* 67, 4812 (1977).
- ⁶P. Hansen and I. R. McDonald, *Theory of Simple Liquids* (Academic, London, 1976), Sec. 6.7.
- ⁷Although the square well is a less realistic potential than the Lennard-Jones form, it may provide the basis for fruitful comparisons. See, for example, J. D. Weeks, D. Chandler, and H. C. Anderson, *J. Chem. Phys.* 54, 5237 (1971), which notes that the square well has less difference in the rapidity of spatial variation, between the attractive and repulsive parts, than the Lennard-Jones potential has: One way to help determine whether some given feature of fluid behavior depends on that type of difference is to compare square-well results with Lennard-Jones results.
- ⁸See, for example, Ref. 6, Sec. 6.3.
- ⁹D. D. Carley, *J. Chem. Phys.* 67, 1267 (1977).
- ¹⁰M. Chen, D. Henderson, and J. A. Barker, *Can. J. Phys.* 47, 2009 (1969).